Recollision Dynamics and Phase Diagram for Nonsequential Double Ionization with Circularly Polarized Laser Fields

L. B. Fu,[1,2] G. G. Xin,[3,4] D. F. Ye,[1] and J. Liu[1,2,3]

[1]*National Laboratory of Science and Technology on Computational Physics, Institute of Applied Physics and Computational Mathematics, Beijing 100088, China*

[2]*Center for Applied Physics and Technology, Peking University, Beijing 100084, China*

[3]*School of Science, Beijing Institute of Technology, Beijing 100081, China*

[4]*Department of Physics, Northwest University, Xian, Shaanxi 710069, China*

(Received 20 September 2011; published 7 March 2012)

A semiclassical quasistatic model is used to investigate the recollision dynamics in circularly polarized laser fields. A velocity window for recollision to occur is found. Only when the return electron's orbits are irregular does significant double ionization take place. The model reproduces the experimental results for magnesium and explains the apparently conflicting experimental results in terms of an analytical formula that demarcates the phase diagram for the nonsequential double ionization in circularly polarized laser fields.

DOI: 10.1103/PhysRevLett.108.103601 PACS numbers: 42.50.Hz, 32.80.Rm, 33.80.Rv, 34.80.Gs

Recollision, i.e., the phenomenon that the released electron can collide under intense laser force with the core, is at the heart of strong-field physics. It is responsible for above-threshold ionization, high-order harmonic generation, etc., and provides unprecedented access to the inner workings of atoms and molecules [1]. The recollision dynamics for nonsequential double ionization (NSDI) is of particular theoretical interest because it provides a model for the study of field-induced electron-electron (e-e) correlation and the three-body Coulomb problem [2–4]. It is commonly believed that NSDI will be significantly suppressed in circularly polarized (CP) fields because a transverse drift velocity due to the rotating electric field causes the electron to spiral away from the core, prohibiting the recollision and NSDI. This picture has been verified by experiments for helium and xenon [5], but not for others such as magnesium [6], NO, and O_2 [7], with the latter showing evidence of NSDI in CP fields. The conflicting evidence between the experiments has motivated some classical simulations [8,9], which indicate that ~6% of the trajectories are subject to recollision in pure CP fields. The double ionization (DI) yields in the knee regime, as calculated from the classical model, however, are 1 order of magnitude larger than that in the experiment [6,9]. Considering that the NSDI is in the quantum tunneling regime [10], investigation of the NSDI mechanism requires a model beyond the pure classical description.

In this Letter, we investigate double ionization in CP laser fields using a semiclassical quasistatic model, where quantum tunneling dynamics is included in the ionization process. Our model calculation reproduces the experimental results for magnesium quantitatively for the first time and explains the apparently conflicting experiments (see Fig. 1). Using the semiclassical model, we investigate the subcycle dynamics of the correlated electrons and obtain a phase diagram for the NSDI in CP fields.

Model calculation.—In our 3D semiclassical quasistatic model [11,12], an electron is released at the outer edge of the barrier. Its exit point in space and time and the initial velocity distribution is exactly determined by the semiclassical theory. The bound electron is allowed to tunnel through the potential barrier with a probability given by the WKB approximation whenever it reaches the outer turning point [13,14]. In comparison to the classical models [8,9], the present semiclassical model depicts the initial tunneling of the outer electron exactly and permits the excited electron to tunnel out in the ionization dynamics.

The exit point is determined by the effective potential in parabolic coordinates (atomic units are used throughout this Letter unless otherwise specified) [15]: $U(\eta) = -1/4\eta - 1/8\eta^2 - \epsilon(t)\eta/8 = -I_p/4$. I_p is the first

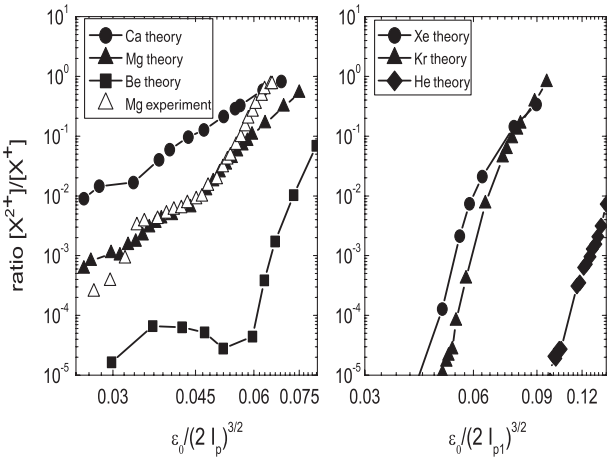

FIG. 1. Our model calculation on the ratios of double- over single-ion yield with respect to the scaled field strength. For the alkaline earth metal atoms, apparent knee structures emerge as the signature of NSDI, while, for the rare gas atoms, knee structures are absent. Experimental data are from Ref. [6].

ionization energy of the atom, and η is the parabolic coordinate relating to the Cartesian coordinate through $\eta \approx -2x$, with the positive x direction assumed to be the instantaneous polarization direction. Solving the $U(\eta)$ equation gives η_0, and the exit point is $(-\eta_0/2, 0, 0)$ in Cartesian coordinates. The above potential predicts an over-the-barrier threshold field $\epsilon_{\text{th}} = I_p^2/2$.

According to the semiclassical theory, the tunneled electron has zero longitudinal velocity and a Gaussian distribution of the transverse velocity [16] $F(v_t) = \exp[-\sqrt{2I_p}v_t^2/|\epsilon(t)|]$, where $\boldsymbol{\epsilon}(t) = \epsilon_0 f(t)[\cos(\omega t)\hat{e}_x + \sin(\omega t)\hat{e}_y]$ denotes the CP field, with ϵ_0 and ω being the amplitude and frequency of the electric field, respectively, and $f(t)$ being the envelope of the pulse that has a constant amplitude for the first ten cycles and turns off with a three-cycle ramp. We consider the potential for the valence electron-nucleus interaction as $V_{\text{ne}}^i = -[(Z-2)s(r) + 2]/|\mathbf{r}_i|$, in which $s(r) = [H(e^{r/d} - 1) + 1]^{-1}$ is the screen function [17] depicting the effect of the multielectron core, Z is the nuclear charge, and H and d are two parameters. For the bound electron, the initial position and momentum are sampled from microcanonical distribution [18]. The subsequent evolution of the two valence electrons with the above initial conditions is governed by Newton's equations.

The ratios of double- over single-ion yields at different field strengths are calculated and shown in Fig. 1. The laser wavelength is chosen as 800 nm to match the experiment [6]. As shown in Fig. 1, our model calculation agrees with the existing experiments and even reproduces the experimental results for Mg quantitatively. We find that the valence-core interaction described by the screening potentials is important in quantitatively reproducing the experimental data. We compare the result from the screening potential with that from the Coulomb potential, and find that the double ionization yields calculated from the screening potential are larger by 1 order of magnitude. This is because the screening potential is wider than the Coulomb potential, and the struck electron is readily excited by the recollision.

Correlated dynamics.—To investigate the recollision dynamics, we use a rotating frame (u, v, w) in which the laser field becomes a static electric field in the u direction with constant strength of ϵ_0. The equations for the outer electron in the rotating frame are $\ddot{u}(t) + 2\omega\dot{v}(t) = -\frac{\partial\Omega}{\partial u}$, $\ddot{v}(t) - 2\omega\dot{u}(t) = -\frac{\partial\Omega}{\partial v}$, and $\ddot{w}(t) = -\frac{\partial\Omega}{\partial w}$, where $\Omega = -\frac{1}{r} - \frac{1}{2}\omega^2 r^2 + \epsilon_0 u$ is the effective potential energy and $r(t) = \sqrt{x(t)^2 + y(t)^2 + z(t)^2} = \sqrt{u(t)^2 + v(t)^2 + w(t)^2}$. The electron experiences two more forces in addition to the Coulomb potential, namely, the centrifugal force $\omega^2\mathbf{r} = \boldsymbol{\nabla}\frac{1}{2}\omega^2 r^2$ and the Coriolis force $2\boldsymbol{\omega} \times \dot{\boldsymbol{\sigma}}$ ($\boldsymbol{\omega} = \omega\hat{\boldsymbol{e}}_z$); $\dot{\boldsymbol{\sigma}} = (\dot{u}, \dot{v}, \dot{w})$ is the electron velocity in the rotating frame. The system has a conserved quantity, the so-called Jaccobi integral [19], $J = \frac{\dot{\boldsymbol{\sigma}}^2}{2} + \Omega$. We project potential function Ω onto the plane of (u, v) and plot it in Fig. 2(a). The parent ion is located at the origin, forming a deep well. The maximum of the potential is located on the positive u axis. On the negative u axis, there is a saddle point, through which the electron can be released via quantum tunneling.

Tracing back the DI trajectories in the knee regime, we find that some tunneled electrons climb up the barrier of effective potential and enter the core regime, interact with the bound electron, and successively trigger NSDI, as shown in Fig. 2(a). In the CP case, the recollision is weak because the return energy is usually small and not enough to knock out the inner electron whose bound energy is about 0.55 a.u. The valence electrons interact with each other through multiple collisions, one electron then emits first, and the other becomes excited and later ionized by the laser field with a long time delay after the recollision [see Fig. 2(b)].

The above picture is more clearly revealed by the calculations on recollision times (t_r), ionization times [Fig. 2(c)], and time delays [Fig. 2(d)]. It is shown that the released electrons return to the core in about 1.3 optical cycles after tunneling, implying that the electrons will spiral back into the third quadrant, as shown in Fig. 2(a). The distribution of the time delays between the ionization of two electrons is much wider, indicating that collision excitation becomes an important channel in the ionization of the second electron. In contrast, the time delay is usually

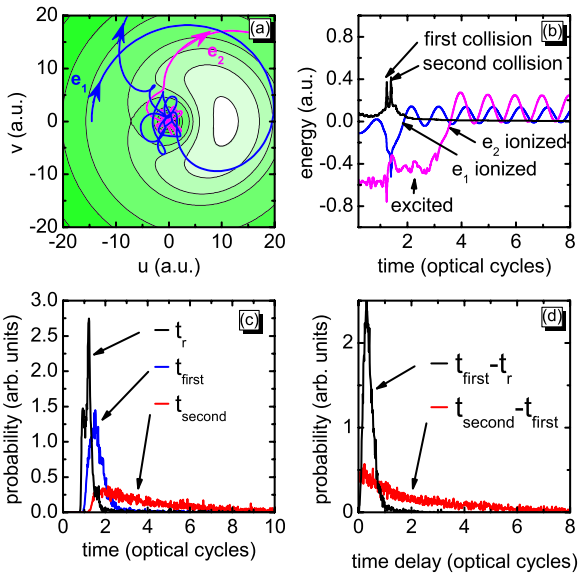

FIG. 2 (color online). (a) Contour plot of the potential Ω and typical NSDI trajectories. The tunneled and bound electrons are colored in blue and light purple, respectively. (b) Temporal evolution of the electron energies and Coulomb repulsive energy $1/r_{12}$; the latter is colored in black. (c) Statistical analysis on recollision and ionization times. The time zero point in (b),(c) is the moment when the tunneled electron releases. (d) Statistical analysis on time delays. The calculation is made for Mg with the laser parameters of 0.02 PW/cm^2 and 800 nm.

small in linearly polarized (LP) fields where the collision is strong and DI occurs soon after the recollision [20,21]. The large time-delay trajectories observed here are somewhat similar to the long quantum orbits responsible for double ionization in elliptic polarized fields [10].

Return window—In CP fields, the classical scenario [22] indicates that the electron released along the negative field direction will have a drift velocity ($v_{\rm drift} = \epsilon_0/\omega$) perpendicular to the instantaneous polarized field direction and cause the electron to spiral out of its parent ion without return. When the drift velocity can be compensated by initial transverse velocity, the recollision will revive [8,9,23]. In our semiclassical model, the tunneled electron has an initial transverse velocity satisfying a Gaussian distribution. We thus expect that there is a window for the initial transverse velocity, in which the tunneled electrons can revisit their parent ion by Coulomb attraction. The above picture is confirmed by our calculation on the recollision distance based on the 2D effective potential model in the rotating frame. Figure 3(a) shows that, when the initial transverse velocities fall into a window with left boundary $v_L \simeq 0.4\epsilon_0/\omega$ and right boundary $v_R \simeq 1.7\epsilon_0/\omega$, the tunneled electrons return with a minimum distance less than 4 a.u., i.e., the range of the inner bounded electron. Interestingly, the window is wide and its width (scaled as ϵ_0/ω) increases with higher field frequency and decreases with larger field strength. A narrow window for the first ionization time was found to associate with DI in the classical model [8]. In our semiclassical model, the transverse velocity distribution, instead of the first ionization time, becomes essential for successful NSDI. Note that the wide window does not necessarily lead to high return probability because each return event is weighed by the Gaussian distribution. In the knee regime for Mg, approximately 2% of the released electrons return.

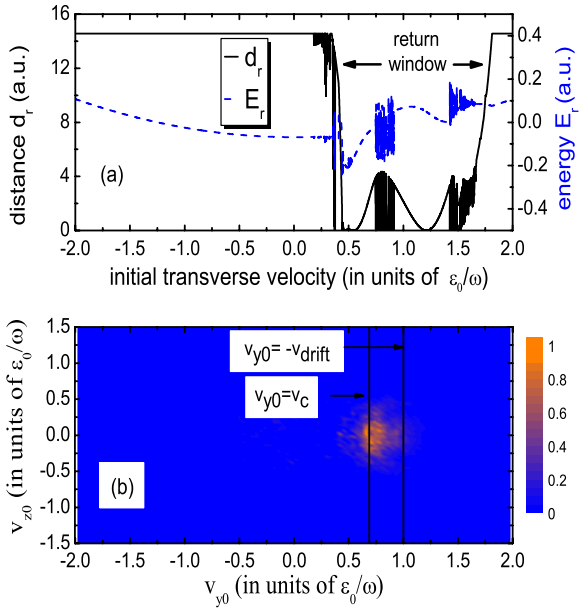

FIG. 3 (color online). (a) The recollision distance and return energy with respect to the initial transverse velocity of the tunneled electrons. (b) Initial velocity distribution that induces the double ionization. The instantaneous polarized field direction is set along the positive x. The calculation is made for Mg with laser parameters of 0.02 PW/cm^2 and 800 nm.

Besides the drift velocity, the system has another characteristic velocity, namely, the critical velocity v_c. When the initial transverse velocity of the tunneled electron is above the critical velocity, it is capable of overcoming the potential hump. The tunneled electron has an initial transverse velocity $\dot{u}(0) = v_0 + \omega\eta_0/2$ and exit point η_0 given by $\eta_0 \approx (I_p + \sqrt{I_p^2 - 2\epsilon_0})/\epsilon_0$. The second term is from the rotating coordinate. Equating the electron's energy $J = \dot{u}^2(0)/2 + \Omega_0$ with the maximum effective potential $\Omega_{\rm max}$, we set up a critical velocity, $v_c = \sqrt{2(\Omega_{\rm max} - \Omega_0)} - \omega\eta_0/2$, with $\Omega_0 = -2/\eta_0 - \omega^2\eta_0^2/8 - \epsilon_0\eta_0/2$ and $\Omega_{\rm max} \approx -\omega^2/\epsilon_0 + \epsilon_0^2/2\omega^2$.

Comparing Figs. 3(a) and 3(b), we see that the velocity window is divided into three regimes according to the two characteristic velocities. In the regime $[v_L, v_c]$, the return energy [24] is small, and it is hard to ionize or even excite the inner electron, while the weight of each DI event is high in this regime because of relatively small velocity values. In the regime $[v_{\rm drift}, v_R]$, the return energy of the tunneled electron is large. It can directly ionize the inner electron through hard collision. However, the weight of each DI event is very small because of the exponential decay of the transverse velocity distribution. It slightly contributes to the total DI yield. This explains why we observe few DI trajectories with small time delay, as indicated in Fig. 2(d). The DI events in our model calculation mainly fall into the regime $[v_c, v_{\rm drift}]$. More interestingly, we observe an unresolved regime, and successive magnifications of the regime exhibit self-similar structures. This type of singular structure is a signal for chaotic scattering [25] of the released electron mediated by the Coulomb and the oscillating laser fields. It is analogous to the phase-dependent single-ionization energy spectrum in LP fields [11]. Dynamically, the released electron wanders chaotically between the stable and unstable manifolds in the phase space and gains energy from the laser field, giving rise to higher return energy. Moreover, the chaotic motion is associated with broadband frequency spectra that can resonantly excite the inner electron through stochastic resonance excitation [26]. The irregular orbits were found to account for the higher above-threshold energy spectra [11] as well as the high-order harmonic generation [27]. It is evident that this chaotic scattering assisted collision excitation ionization contributes significantly to the NSDI.

Phase diagram.—According to the semiclassical model, the ratios of double- over single-ion yield can be approximately expressed as $[X^{2+}]/[X^+] \simeq \frac{1}{10}\frac{\int^{\Delta_{\rm win}} F(v_t)dv_t}{\int_0^{\infty} F(v_t)dv_t}$, where $F(v_t)$ is the Gaussian distribution on traversal velocity,

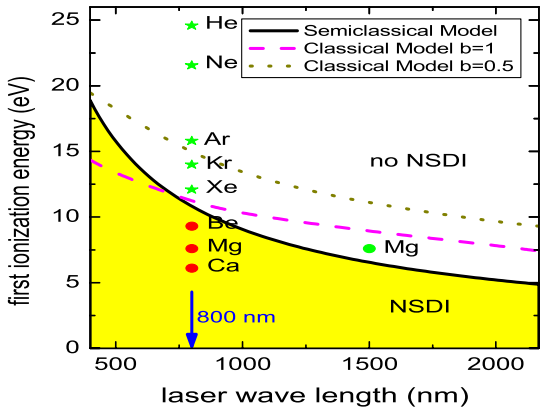

FIG. 4 (color online). Phase diagram for NSDI in CP fields. The solid and dashed (dotted) lines are the demarcation lines from semiclassical and classical models, respectively. The red circles indicate the NSDI signal presence in our semiclassical ensemble simulation, while the green stars indicate no NSDI signal presence.

Δ_{win} is the recollision window, and the prefactor $1/10$ accounts for the fact that only one-tenth of the return trajectories can successively trigger NSDI. Considering that the NSDI emerges mainly around critical velocity v_c and the width of the recollision window approximates to ϵ_0/ω, the above expression reduces to [28] $[X^{2+}]/[X^{+}] \simeq \frac{(2I_p^5)^{1/4}}{10\sqrt{\pi\omega}} \exp[-I_p^{5/2}/2\sqrt{2}\omega^2]$. In the above deduction, the typical field strength, i.e., $\epsilon_0 = \epsilon_{\mathrm{th}}/2 = I_p^2/4$, and long wavelength limit of $\omega \to 0$ are exploited. We then can obtain an explicit expression for the NSDI criterion as $\omega \approx 0.18(I_p)^{5/4}$, which corresponds to a ratio of 10^{-5} for the double-to-single ionization yield. Below it, the double ionization events are too few to be detectable in the experiments. The analytic result is plotted in Fig. 4.

We also put on the rare gas atoms and alkali metal atoms in Fig. 4 at an experimental laser wavelength of 800 nm. It is clearly seen that all the rare gas atoms are above the semiclassical criterion and the alkaline metal atoms are below it, consistent with the existing experiments and our model calculation. The phase diagram exhibits the laser wavelength dependence of NSDI, as confirmed by our numerical simulation. For example, if we shift the laser wavelength to 1500 nm, our model calculation exhibits that, for the Mg atom, the knee structure disappears.

In the completely classical model, both valence electrons are set initially on the energy shell with ground energy E_g [9]. When laser fields apply, one electron might get ionized through the over-the-barrier trajectories and double ionization most likely occurs when the ionized electron revisits the core and collides with the second electron. Hence, one can get a heuristic criterion for the recollision: $p_{\max} \sim \epsilon_0/\omega$, where $p_{\max} = \sqrt{2(E_g - \frac{1}{a} + \frac{8}{\sqrt{5a^2-b^2}})}$ is the maximum admissible classical momentum for ground-state energy E_g, and a and b are the parameters used in the soft Coulomb potentials for electron-nuclear and electron-electron, respectively. The relation between the parameters satisfies $E_g = -\frac{4}{a} + \frac{1}{b}$. The minus ground energy can be approximately regarded as the sum of the first (I_p) and the second (I_p') ionization potentials. With using an approximate relation between the first ionization potential and the second ionization potential, i.e., $I_p' = 2I_p$, , we can obtain the classical boundary expression as [28] $\omega = \frac{I_p^2}{4}\sqrt{2(\frac{8(1+3bI_p)}{b\sqrt{80-(1+3bI_p)^2}} - \frac{15I_p}{4} - \frac{1}{4b})}$.

The demarcation lines from the classical model depend on the soft parameter b and shift upward dramatically with decreasing the parameter, as shown in Fig. 4. The specific choice of $b = 1$ is exploited in the simulation [9]. The classical theory deviates largely from the semiclassical result. For instance, at the long wavelength of 1500 nm, the classical theory predicts that, for the Mg atom, the knee structure should emerge as the signal of NSDI. The deviation may be partly due to the fact that the completely classical model has largely overestimated the recollision probability and the NSDI yields accordingly [6,9].

In summary, with a semiclassical model, we achieve insight into the recollision dynamics for NSDI with CP laser fields. We find a velocity window for the recollision to occur and unveil the important role of the chaotic return electrons in triggering NSDI. We obtain an analytical formula that demarcates the phase diagram for the NSDI and compare it with that from the completely classical model. The present theory should encourage further experimental verification of the predicted NSDI properties in the light of the classicality or nonclassicality of NSDI in CP fields.

This work is supported by the NFRP (2011CB921503) and the NNSF of China (Grants No. 10725521, No. 11075020, and No. 91021021).

[1] P. B. Corkum, Phys. Today **64**, 36 (2011).
[2] P. B. Corkum, Phys. Rev. Lett. **71**, 1994 (1993).
[3] W. Becker and H. Rottke, Contemp. Phys. **49**, 199 (2008).
[4] C. Figueira de Morisson Fariaa and X. Liu, J. Mod. Opt. **58**, 1076 (2011), and references therein.
[5] B. Walker *et al.*, Phys. Rev. A **48**, R894 (1993).
[6] G. D. Gillen, M. A. Walker, and L. D. VanWoerkom, Phys. Rev. A **64**, 043413 (2001).
[7] C. Guo and G. N. Gibson, Phys. Rev. A **63**, 040701(R) (2001); C. Guo *et al.*, *ibid.* **58**, R4271 (1998).
[8] Xu Wang and J. H. Eberly, Phys. Rev. Lett. **105**, 083001 (2010).
[9] F. Mauger, C. Chandre, and T. Uzer, Phys. Rev. Lett. **105**, 083002 (2010).
[10] N. I. Shvetsov-Shilovski, S. P. Goreslavski, S. V. Popruzhenko, and W. Becker, Phys. Rev. A **77**, 063405 (2008).

[11] Bambi Hu, Jie Liu, and Shi-Gang Chen, Phys. Lett. A **236**, 533 (1997).
[12] Li-Bin Fu, Jie Liu, Jing Chen, and Shi-Gang Chen, Phys. Rev. A **63**, 043416 (2001).
[13] J. S. Cohen, Phys. Rev. A **64**, 043412 (2001).
[14] D. F. Ye and J. Liu, Phys. Rev. A **81**, 043402 (2010).
[15] L. D. Landau and E. M. Lifshitz, *Quantum Mechanics* (Pergamon, New York, 1977).
[16] N. B. Delone and V. P. Krainov, J. Opt. Soc. Am. B **8**, 1207 (1991).
[17] P. P. Szydlik and A. E. S. Green, Phys. Rev. A **9**, 1885 (1974).
[18] R. Abrines and I. C. Percival, Proc. Phys. Soc. London **88**, 861 (1966); J. G. Leopold and I. C. Percival, J. Phys. B **12**, 709 (1979).
[19] In the retsricted three-body problem, the field term is replaced by the gravity potential of the second primary body. See V. G. Szebehely, *Theory of Orbits* (Academic, New York, 1967).
[20] S. L. Haan *et al.*, Phys. Rev. Lett. **97**, 103008 (2006).
[21] S. L. Haan *et al.*, Opt. Express **15**, 767 (2007); D. F. Ye, J. Chen, and J. Liu, Phys. Rev. A **77**, 013403 (2008).
[22] P. B. Corkum, N. H. Burnett, and F. Brunel, Phys. Rev. Lett. **62**, 1259 (1989).
[23] R. Kopold, D. B. Milosevic, and W. Becker, Phys. Rev. Lett. **84**, 3831 (2000).
[24] The return energy is the sum of kinetic energy and core potential, rather than the return kinetic energy, as in the LP case. This is because, in the CP case, return emerges only under the assistance of core attraction; in this situation, return kinetic energy is not well defined.
[25] Y. C. Lai and T. Tél, Applied mathematical sciences **173**, 187 (2011).
[26] L. Gammaitoni *et al.*, Rev. Mod. Phys. **70**, 223 (1998).
[27] G. van de Sand and J. M. Rost, Phys. Rev. Lett. **83**, 524 (1999).
[28] See Supplemental Material at http://link.aps.org/supplemental/10.1103/PhysRevLett.108.103601 for more details.